# FORMATION PROCESS OF EMPTY AND METAL-CONTAINING FULLERENE —MOLECULAR DYNAMICS AND FT-ICR STUDIES—

Shigeo Maruyama[a]*, Yasutaka Yamaguchi[a], Masamichi Kohno[b] and Tetsuya Yoshida[a]

[a] *Department of Mechanical Engineering and* [b] *Engineering Research Institute, The University of Tokyo, Tokyo, Japan*

**ABSTRACT** The formation mechanism of empty and metal-containing fullerene was studied through MD (molecular dynamics) simulations and FT-ICR (Fourier transform ion cyclotron resonance) mass spectroscopy of laser vaporized carbon cluster. Multi-body classical potential functions for metal-carbon and metal-metal interactions were constructed based on DFT (density functional theory) calculations of various forms of small clusters $MC_n$ and $M_n$ (M = La, Sc, Ni). Using the modified Brenner potential for carbon-carbon interaction, the clustering process starting from 500 isolated carbon atoms and 5 metal atoms in gas phase was simulated under the controlled temperature condition at 3000K. The difference of clustering process of $La@C_n$, $Sc@C_n$ and $NiC_n$ were compared with empty fullerene formation simulation.

FT-ICR mass spectrometer directly connected to the laser vaporization cluster beam source was implemented in order to experimentally study the clustering process. The increase of cluster nozzle pressure roughly corresponded to the later stage of the molecular dynamics simulation. The FT-ICR mass spectra of metal-carbon composite clusters were compared for various sample

* To whom correspondence should be addressed

materials used for arc-discharge generation of metal-containing fullerene and SWNT (single-wall carbon nanotube); La, Y, Sc, Gd, Ce, Ca, and Ni-Y. Positive La-C, Y-C, Sc-C, Gd-C, Ce-C binary clusters commonly showed strong $MC_{2n}^+$ signal in the range of $36 < 2n$ with intense magic numbers at $MC_{44}^+$, $MC_{50}^+$ and $MC_{60}^+$. It was speculated that the even-numbered clusters corresponded to the annealed random caged clusters observed in the MD simulation.

## INTRODUCTION

After the discovery of $C_{60}$ by Kroto *et al.*[1], macroscopic amount of empty fullerene[2,3], metallofullerenes[4-7], higher fullerenes[8] and carbon nanotubes[9] were successively produced and isolated. Recently, the high quality generation of SWNTs[10,11] has demonstrated new possibilities of applications of this material. Even though the generation of fullerene is now possible by the arc-discharge technique[2,3] or the laser-oven technique[3], the formation mechanism of such spherical molecules is not clear.

We have performed MD simulations of the clustering process of carbon atoms to investigate the fullerene formation mechanism[12,13], and the temperature dependence of the cluster structures was observed[12]. In addition, we have demonstrated the formation of perfect $C_{60}$ structure by giving sufficient collision-free annealing time, and examined the time and temperature scale of the annealing process through the reaction rate of the network transformations. Based on these results, a new formation model of empty fullerene including the temperature effect was proposed[13].

In spite of possible interesting applications of metallofullerene, it is still difficult to obtain macroscopic amount of sample because of extremely low yield of generation. In order to find the optimum generation condition, it is inevitable to understand the formation mechanism. According to experimental studies, the metal atoms such as La, Y, Sc, Ca and lanthanide can be enclosed inside the carbon cage, and the preferred carbon cage structure depends on the metal. On the other hand, Ni, Co, or Fe, which are not experimentally assigned to be encapsulated in the fullerene cage, are required to generate the SWNTs[10,11]. Here, the role of these metal atoms on the carbon cluster growth process is still

unknown. In this paper, the formation process of metallofullerene is studied by using the MD simulations and FT-ICR mass spectrometry of metal-carbon binary clusters generated by the laser-vaporization supersonic-expansion cluster beam source.

## MOLECULAR DYNAMICS SIMULATION

The principal technique of the classical MD simulation is the same as our previous simulations[12,13] of pure carbon system using the modified Brenner potential[14]. In addition, we have constructed the potential function between metal-carbon and metal-metal potential function[15,16], based on the calculations of the binding energy and charge state of various forms of small clusters $MC_n$ and $M_n$ (M: La, Sc, Ni). Here the density functional theory (DFT) based on the Becke's three-parameter exchange functional[17] with the Lee-Yang-Parr correlation[18] (B3LYP) was applied with the effective core potentials derived from the LANL2DZ basis from Gaussian 94[19].

The multi-body potentials between metal-carbon potential functions were constructed as functions of carbon coordinate number of a metal atom. The total potential energy was expressed as the sum of binding energy $E_b$ as follows.

$$E_b = V_R + V_A + V_C \tag{1}$$

$$V_R = f(r_{ij}) \frac{D_e}{S-1} \exp\left\{-\beta\sqrt{2S}(r_{ij} - R_e)\right\} \tag{2}$$

$$V_A = -f(r_{ij}) \cdot B^*_{ij} \frac{D_e S}{S-1} \exp\left\{-\beta\sqrt{2/S}(r_{ij} - R_e)\right\} \tag{3}$$

$$V_C = -f(r_{ij}) \frac{e^2}{4\pi\varepsilon_0} \frac{c_C c_M}{r_{ij}} \tag{4}$$

Here, $r_{ij}$, $V_R$ and $V_A$ denote the distance between metal $i$ and carbon $j$, Morse-type repulsive and attractive terms, respectively. The Coulomb term $V_C$ is applied only to the La-C and Sc-C interactions that were calculated to be strongly ionic due to the electron transfer from the metal to carbon atoms. The coordinate number of the metal atom $N^C$ is defined and both the additional term $B^*_{ij}$ and electric charge $c_C$ and $c_M$ of carbon and metal are expressed as functions of the coordinate number. Here, the cut-off function $f(r)$ and parameter constants $\beta$, $S$, $R$e are

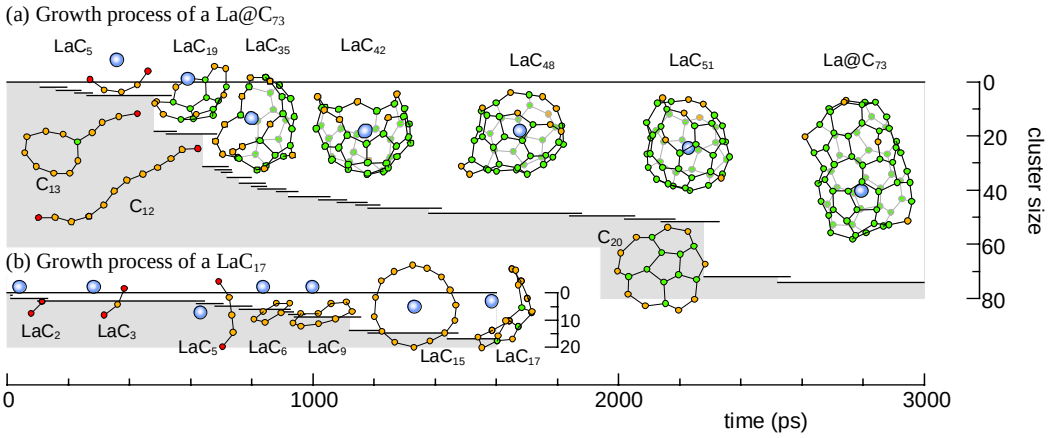


FIG. 1 Growth process of La attached clusters: (a) La@$C_{73}$ and (b) La@$C_{17}$.

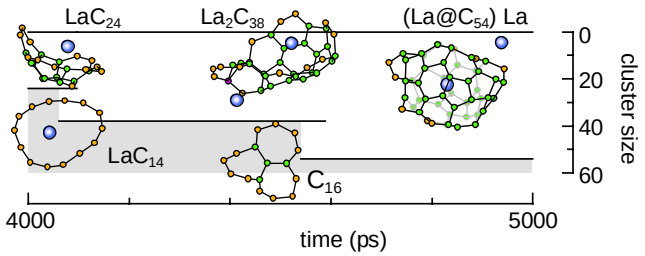


FIG. 2. Collision of La attached clusters.

described elsewhere[15,16]. Metal-metal interactions were constructed[15,16] in the same formula as in eq. (1). In this case, the equilibrium binding energy $D_e$ and the bond length $R_e$ are expressed as direct functions of the metal coordinate number instead of using the additional term $B^*_{ij}$ in eq. (3). The temperature control method and the integration techniques were fully described in our previous report[12].

## RESULTS OF MOLECULAR DYNAMICS SIMULATIONS

### Lanthanum-carbon system

Five hundred carbon atoms and 5 La atoms in gas phase with random positions and velocities were distributed in a 342 Å cubic box with fully periodic boundary condition. The system was controlled toward a control temperature $T_c$ of 3000K. These parameters corresponded to the condition in which $C_{60}$ and $C_{70}$ caged clusters were obtained in the simulation without including metal atoms[12].

FIG. 1 shows the growth process of typical La attached clusters in the simulation; (a) a La containing caged cluster La@$C_{73}$ observed at $t$ = 3000 ps, and (b) a La attached cluster $LaC_{17}$ observed at $t$ = 1600 ps. The vertical width and horizontal length denote the cluster size and time, respectively. For example, in FIG. 1(a), the $LaC_5$ and $C_{13}$ cluster independently existed each other, coalesced at about 530 ps, and the $LaC_{19}$ was formed after the addition of a carbon atom at about 550 ps.

The remarkable difference from our simulation for empty fullerene[12] was clearly observed in the precursors in the size range of $LaC_{19}$ to $LaC_{51}$. Since the La atom can be a nice nucleation site of carbon atoms, it can attract carbon atoms by Coulomb force in very much organized manner. The open-cap appearance of carbon cluster form resembles to the 'pentagon road' fullerene formation model[3] proposed for empty fullerene. The cluster grew larger with closing the open-cap structure after $LaC_{51}$. In this case, however, a collision with a large cluster of $C_{20}$ prevented gradual growth and resulted in the formation of a caged cluster larger than La@$C_{71}$, and the La atom was almost encapsulated in the carbon cage. Considering the difference of time and temperature scale between the real phenomena and simulation[13], these hollow caged structures could have sufficient collision free annealing interval to form more sophisticated structures.

FIG. 2 shows a collision process of two clusters each of that has a La atom. In this case, two lanthanum atoms could not attach on the same face of the flat structure during the coalescence process due to the Coulomb repulsion, and that resulted in the encapsulation of only one La atom: La(La@$C_{54}$).

**Scandium-carbon system**

Clustering process with Sc atoms was simulated under the same condition as the previous section. FIG. 3 shows the growth process of a $ScC_{55}$ observed at $t$ = 4000 ps. A remarkable difference of the process from La-C system is apparent for the structures of $MC_n$ ($20<n<40$) because of the weaker Coulomb force. The cluster annealed to the 3-dimensional open cage structure around $ScC_{43}$, where the scandium atom moved around the open edge. The Sc atom slipped into the caged structure just before closing at around Sc@$C_{54}$. The random caged form of carbon

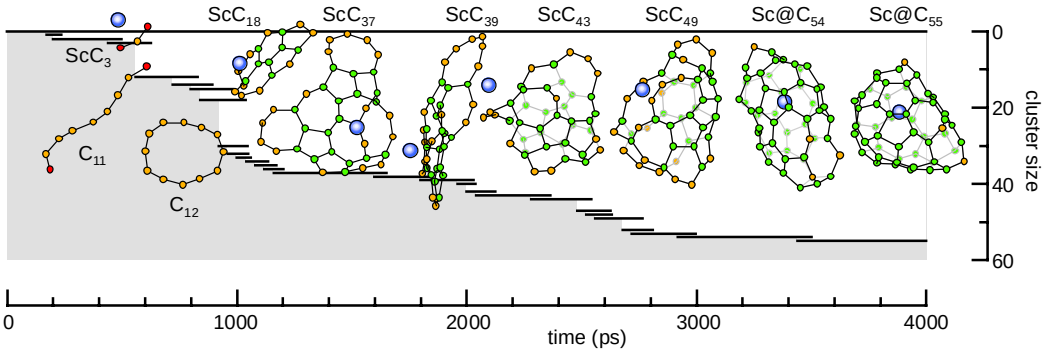


FIG. 3 Growth process of a Sc attached cluster $Sc@C_{55}$.

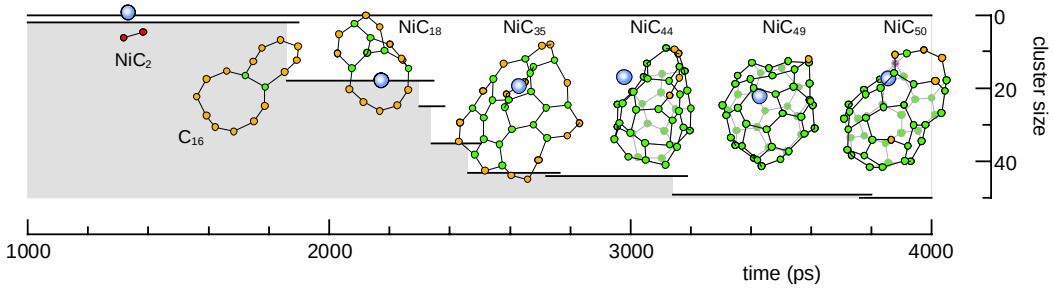


FIG. 4 Growth process of a Ni attached cluster $NiC_{50}$.

clusters is almost the same as the case of our empty fullerene simulation[12]. The effect of Sc atom is relatively weak to change the carbon structure.

In addition to this final stage of encapsulation, the flat structures around $ScC_{35}$ maybe related to the possibility of catching another Sc atom, which is in good agreement with experimentally observed prominence of di-metallofullerene for Sc-C system.

**Nickel-carbon system**

Nickel atom, which is not experimentally assigned to be encapsulated in the fullerene cage so far, is also examined. As shown in FIG. 4, the growth process is very similar to that for Sc attached cluster. However, at the final stage, the Ni atom preferred to attach at the large defect of the caged structure such as large rings of more than 7 or 8 membered, and frequently moved in and out of the carbon cage. FIG. 5 shows the similar motion also observed for a larger caged cluster of $NiC_{78}$ obtained for another Ni atom. Moreover, when two Ni atoms

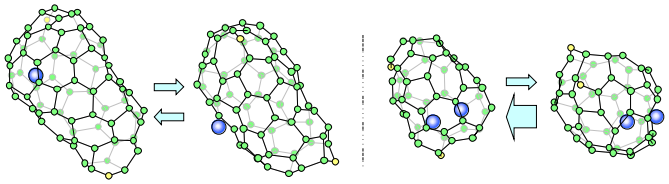

(a) $NiC_{78}$ (b) $Ni_2C_{54}$

FIG. 5 Structures of Ni attached cage clusters: (a) $NiC_{78}$ and (b) $Ni_2C_{54}$.

were enclosed in the host cage as shown in FIG. 5 (b), the Ni atoms remained inside the cage more stably than the case of single Ni atom, and that can be a hint of a new endohedral form of metallofullerene.

## FT-ICR STUDIES OF LASER VAPORIZED CLUSTERS

### FT-ICR mass spectroscopy

The FT-ICR is the unique mass spectroscopy based on the ion-cyclotron motion of clusters in a strong magnetic field. In principle, extremely high mass-resolution at high mass-range such as resolution of 1 amu at 10,000 amu range can be obtained[20]. Furthermore, since the ions can be trapped in the vacuum for a

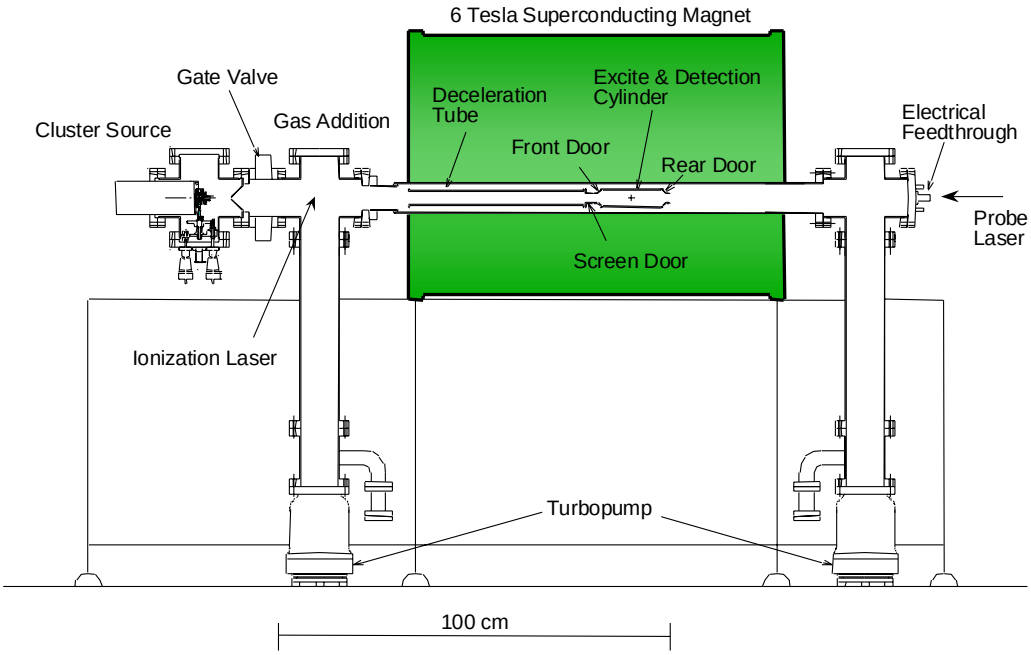


FIG. 6 FT-ICR apparatus with direct injection cluster beam source

few minutes, it is possible to perform laser photo-fragmentation experiments[21] and chemical reaction experiments[22]. We have built a FT-ICR spectrometer with a 5.87 Tesla superconducting magnet[23], based on the similar design concept as our previous version at Rice University[20]. The schematics of the whole apparatus are shown in FIG. 6. The ICR cell 42 mm I.D. 150 mm long cylinder was placed in a stainless tube (SUS316) of 84 mm I.D. which penetrated the homogeneous 5.87 Tesla superconducting magnet commercially available for NMR. Two turbo-pumps (300 $/s$) fore-pumped by a smaller turbo-pump of 50 $/s$ were placed at the floor in order to avoid the effect of strong magnetic field. The typical background pressure was $3\times10^{-10}$ Torr.

The atomic cluster beam was generated outside of magnetic field by the laser-vaporization cluster beam source shown in FIG. 7. The design principle of this cluster source was similar to our previous versions[20,24]. A pulsed gas valve, the sample motion mechanism and a skimmer were installed in a 6-inch 6-way UHV cross. A solid sample disk was vaporized by the focused beam of Nd:YAG

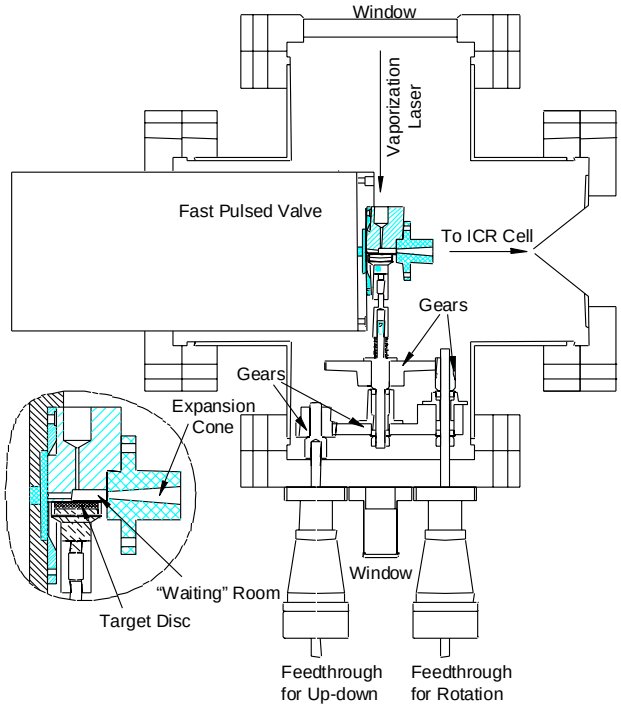


FIG. 7 Supersonic laser-vaporization cluster beam source

laser (2nd Harmonics) while timed pulsed gas was injected to the nozzle. In the atmosphere of helium gas, vaporized atoms condensed to clusters, and then, were carried and cooled by the supersonic expansion of helium gas. An important feature of this cluster source nozzle design is the properly size-adjusted "waiting room" which keeps clusters at relatively high pressure for about 40 μs. The cluster beam was directly injected to the magnetic field through a skimmer with the opening diameter of 2 mm and a deceleration tube[20].

**Laser vaporized carbon clusters**

Examples of carbon mass spectra measured by the direct-injection FT-ICR apparatus are shown in FIG. 8. Here, a graphite sample was vaporized by the laser and the positive carbon clusters were trapped. FIG. 8 (a) is very much similar to the well-known positive carbon mass distribution, which lead to the discovery of spherical $C_{60}$ structures[1]. We can observe completely different aspects of mass spectra for less amount of source helium gas in the nozzle of the

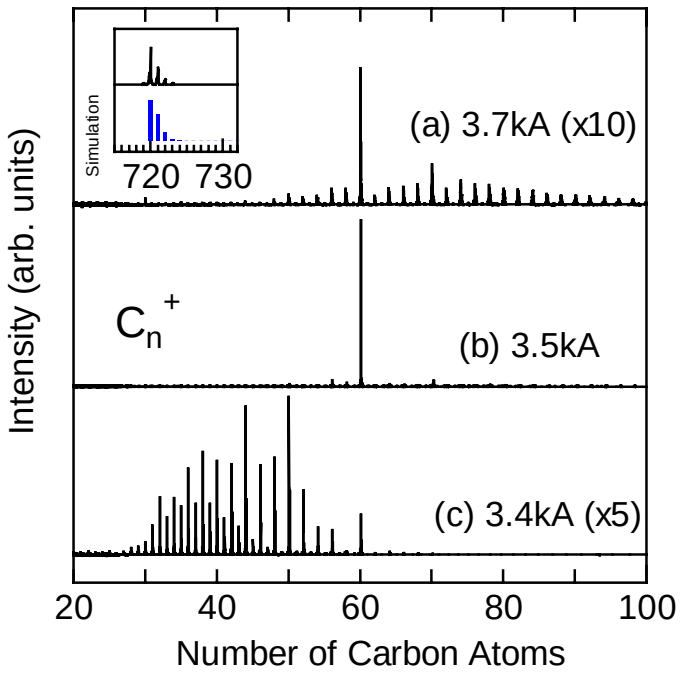


FIG. 8 Dependence of Helium gas pressure on the carbon cluster cation mass distribution.

laser-vaporization cluster source. The driving current of the pulsed nozzle, which was roughly proportional to the nozzle pressure, was changed in FIG. 8. At the condition of FIG. 8 (b) almost only $C_{60}$ was observed and the even less pressure lead to the odd number of carbon atoms, which could be regarded as the non-closed structures of positive carbon clusters. These findings of intermediate stage of the fullerene formation must be very important for understandings of the fullerene formation mechanism. FIG. 8 implies that the decrease of pressure in the nozzle corresponds to the earlier stage of the formation process. It should be noticed that $C_{44}$, $C_{50}$ and $C_{60}$ were observed to be special magic numbers in FIG. 8 (c).

**Metal-carbon binary clusters**

The FT-ICR mass spectra of metal-carbon composite clusters were studied for sample materials used for the arc-discharge generation of metal-containing fullerene and SWNT; La: 0.8%, Y: 0.8%, Sc: 0.8%, Gd: 0.8%, Ce: 0.8%, Ca: 0.3%, and Ni:4.2% & Y: 1%. FIG. 9 shows the positive clusters from various samples. It should be noticed that only a part of the mass range was trapped in the ICR cell. Positive La-C, Y-C, Sc-C, Gd-C, Ce-C binary clusters commonly showed strong $MC_{2n}^{+}$ signal in the range of $36 < 2n$ with intense magic numbers at $MC_{44}^{+}$, $MC_{50}^{+}$ and $MC_{60}^{+}$. The mass-spectroscopic result was very surprising for La-C and Y-C cases, since there was only a trace of pure carbon clusters ($C_{60}$) in FIG. 9. All other clusters had only one metal atom. In the case of Sc-C, on the other hand, the bare carbon clusters exhibited almost the same intensity as binary clusters. If we ignore the metal-composite clusters, the distribution of bare carbon clusters was almost the same as typical positive ion clusters. Almost all of metal-carbon composite clusters had only one metal atom and even number of carbon atoms: $MC_{2n}$ in the range of $36 < 2n$, with special magic numbers of $MC_{44}$, $MC_{50}$, $MC_{60}$ (M = La, Y, Sc, Gd, Ce). For C-Ca case, this feature was still valid but $CaC_{60}$ was very much enhanced. The cases of Gd-C and Ce-C were almost the same as La-C case. These features resembled to the magic number feature observed in FIG. 8 (c) for pure carbon but enhanced with an addition of a metal atom.

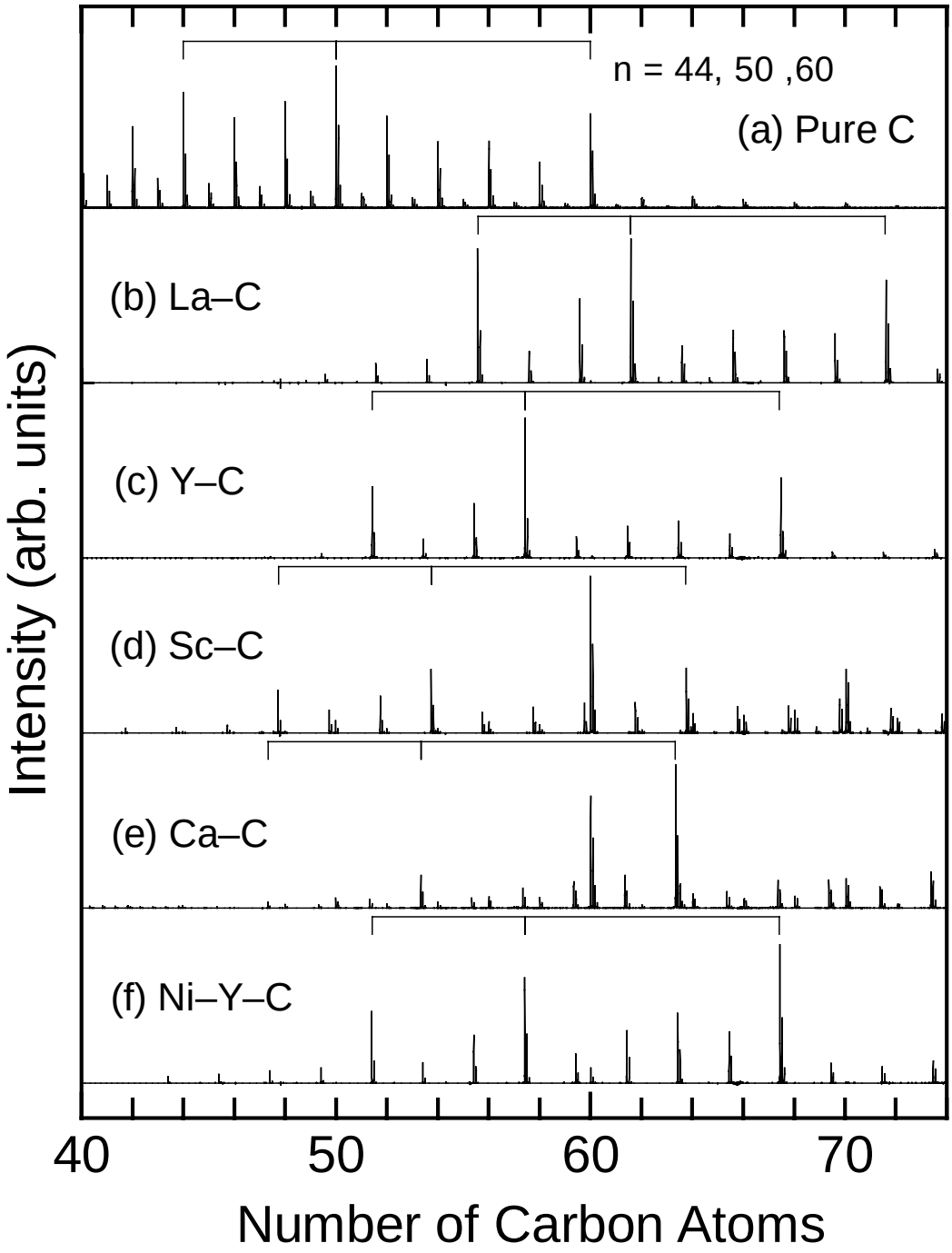


FIG. 9 FT-ICR mass spectra of positive clusters generated by vaporizing various metal-carbon composite materials. (a) Pure Carbon, (b) La 0.8%, (c) Y 0.8%, (d) Sc 0.8%, (e) Ca 0.3%, (f) Ni 4.2% & Y 1%.

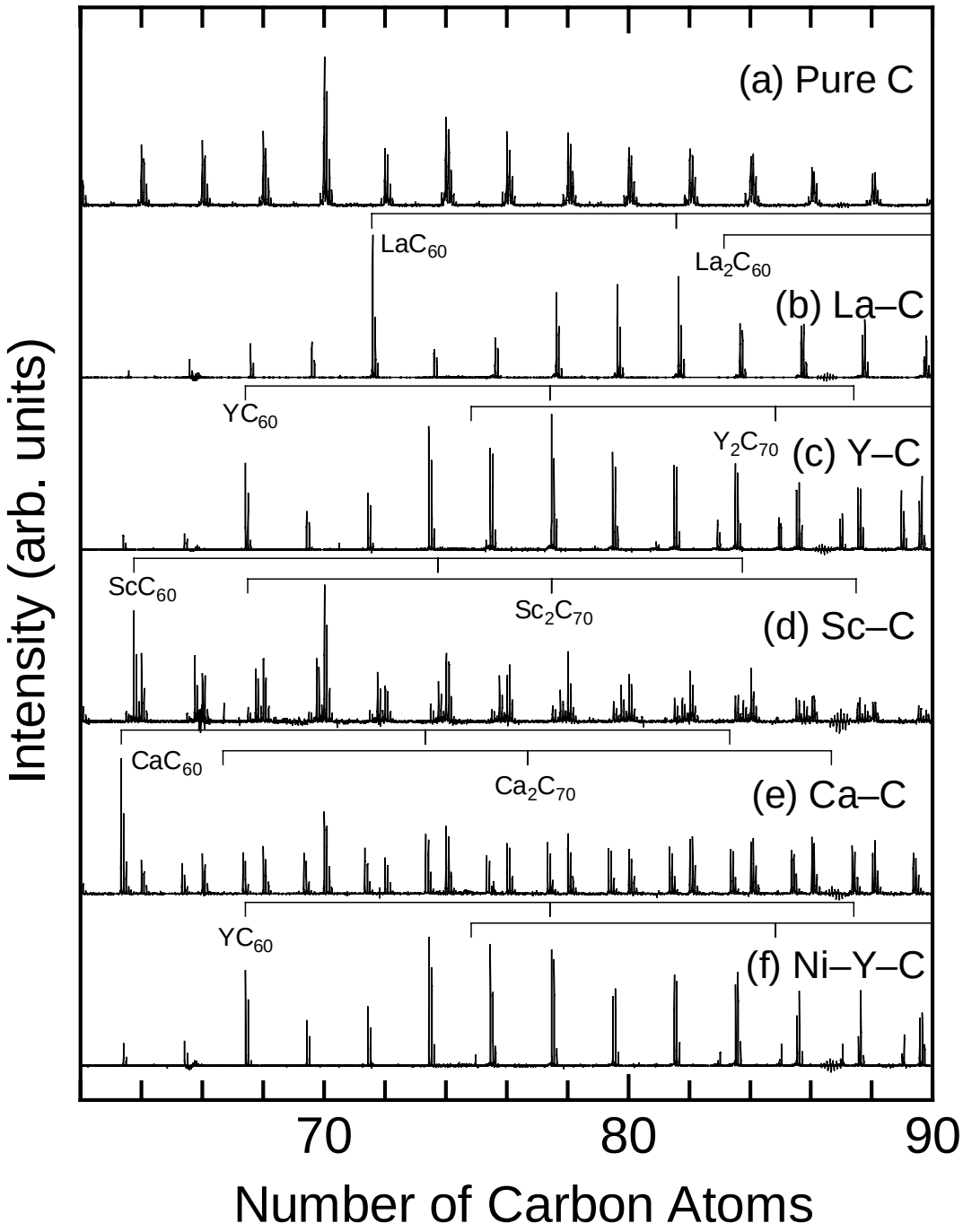


FIG. 10 FT-ICR mass spectra of positive clusters with higher pressure at the nozzle. (a) Pure Carbon, (b) La 0.8%, (c) Y 0.8%, (d) Sc 0.8%, (e) Ca 0.3%, (f) Ni 4.2% & Y 1%. Horizontal bars over each spectrum are masses at $MC_n$, n = 60, 70, 80 and $M_2C_n$, n = 60, 70, 80.

FIG. 10 shows the cluster distributions generated with higher pressure condition at the cluster-source nozzle. Di-metallic clusters were observed only for Y-C and Sc-C systems. There is the clear minimum size of these di-metallic clusters as $Sc_2C_{54}$ and $Y_2C_{64}$.

**Hypothesis of cluster forms observed in mass spectra**

Comparison of MD results and mass-spectroscopy is not straightforward because the time-compressed MD lacked the realistic annealing process, and because the cluster mass-distribution of cluster source is not a snapshot of MD but is reflecting cluster ions surviving the additional collisions with He and each other. In addition, the distribution observed in FIG. 9 and 10 for positive ions are different from those for negative or neutral clusters in general. Nevertheless, some hypothesis can be drawn through comparisons. The complete lack of odd numbered carbon clusters for $MC_n$ with $n > 36$ can be ascribed to the enhancement of clustering process due to the metal atom. The even number of carbon atoms strongly suggests that all of these composite clusters have closed caged structure: according to Euler's theorem for a closed polyhedron, the number of atoms must be even when all atoms have three bonds[13]. We believe that these composite clusters should have imperfect fullerene caged structure with metal atom inside of the cage. The appearance of minimum size of di-metallic clusters in FIG. 10 also supports this hypothesis.

The 44, 50, 60 magic number features for $C_n$ and $MC_n$ are probably related to the stable closed form. MD results in FIG. 1 shows that the carbon cage can be almost closed at about $MC_{44}$ range. This closure is enhanced with the effect of a metal atom that works as the center of organization of the structure.

**Role of metal atoms in the generation of SWNT**

The Ni-Y-C composite material with 4.2% Ni and 1% Y used for the very high yield arc-discharge generation[25] of SWNT was tested by the cluster source as shown in FIG. 9 (f) and FIG. 10 (f). The positive mass spectra were unfortunately exactly the same as for Y-C binary case (FIG. 9 (c), 10(c)). We could find no trace of Ni in positive clusters.

## CONCLUSIONS

Multi-body potential functions of metal-carbon and metal-metal system were constructed based on the *ab initio* calculations of small $MC_n$ and $M_n$ (M: La, Sc, Ni) using the density functional theory. By applying the potential function to the molecular dynamics simulation, the clustering processes starting from randomly distributed carbon and metal atoms were simulated and the formation process of metal attached caged carbon clusters were examined. When La atoms were applied, the stable open-cap structure surrounding the La atom resulted in the lanthanum-containing caged cluster. For Sc-C system, the Sc atom was encapsulated into the host cage at the final stage of the growth process. For Ni-C system, the Ni atom finally stayed on a face of large ring of the caged structure.

We have successfully implemented the FT-ICR mass spectrometer with direct-injection cluster beam source. For bare carbon positive clusters, we found the special condition where the odd-numbered clusters were observed in the range of $C_{30}$ to $C_{50}$ and the continuous change to $C_{60}$-dominant condition and 'normal' even-numbered distribution. The metal-composite clusters showed magic numbers of $MC_{44}$, $MC_{50}$, $MC_{60}$ (M = La, Y, Sc, Gd, Ce). The even-numbered carbon atoms for metallofullerene and the minimum size of di-metallic fullerene strongly suggest that all of these clusters have the caged form with one or two metal atoms inside.

## ACKNOWLEDGEMENTS

This work was supported by Grant-in-Aid for Scientific Research (No. 09450085), Grant-in-Aid for Exploratory Research (No. 10875047) and Grant-in-Aid for JSPS Fellows (No. 08004746) from the Ministry of Education, Science, Sports and Culture, Japan. One of the author (S. M.) thanks Professor R. E. Smalley at Rice University for discussions and his kind support for the superconducting magnet.

## REFERENCES

1. Kroto, H. W., Heath, J. R., O'Brien, S. C., Curl, R. F. and Smalley, R. E., *Nature* **318**, 162 (1985).

2. Krätschmer, W., Lamb, L.D., Fostiropoulos, K. and Huffman, D. R., *Nature* **347**, 354 (1990).
3. Haufler, R. E., Chai, Y., Chibante, L. P. F., Conceicao, J., Jin, C., Wang, L.-S., Maruyama, S. and Smalley, R. E., *Proc. Mat. Res. Soc. Symp.* **206**, 627 (1991).
4. Chai, Y., Guo, T., Jin, C., Haufler, R. E., Chibante, L. P. F., Fure, J., Wang, L., Alford, J. M. and Smalley, R. E., *J. Phys. Chem.* **95**, 7564 (1991).
5. Shinohara, H., Sato, H., Saito, Y., Ohkohchi, M. and Ando, Y., *J. Phys. Chem.* **96**, 3571 (1992).
6. Kikuchi, K., Suzuki, S., Nakano, Y., Nakahara, N., Wakabayashi, T., Shiromaru, H., Saito, K., Ikemoto, I. and Achiba, Y., *Chem. Phys. Lett.* **216**, 23 (1993).
7. Takata, M., Umeda, B., Nishibori, E., Sakata, M., Saito, Y., Ohno, M. and Shinohara, H., *Nature* **377**, 46 (1995).
8. Kikuchi, K., Nakahara, N., Wakabayashi, T., Honda, M., Matsumiya, H., Moriwaki, T., Suzuki, S., Shiromaru, H., Saito, K., Yamauchi, K., Ikemoto, I. and Achiba, Y., *Chem. Phys. Lett.* **188**, 177 (1992).
9. Iijima, S., *Nature* **354**, 56 (1991).
10. Iijima, S., Ichihara, T., *Nature* **363**, 603 (1993).
11. Thess, A., Lee, R., Nikolaev, P., Dai, H., Petit, P., Robert, J., Xu, C., Lee, Y. H., Kim, S. G., Rinzler, A. G., Colbert, D. T., Scuseria, G. E., Tomanak, D., Fischer, J. E. and Smalley, R. E., *Science* **273**, 483 (1996).
12. Yamaguchi, Y. and Maruyama, S., *Chem. Phys. Lett*. **286**, 336 (1998).
13. Maruyama, S. and Yamaguchi, Y., *Chem. Phys. Lett.* **286**, 343 (1998).
14. Brenner, D. W., *Phys. Rev. B* **42**, 9458 (1990).
15. Yamaguchi, Y., Maruyama, S. and Hori, S., *5th ASME/JSME Thermal Eng. Conf.*, San Diego, AJTE99-6508 (1999).
16. Yamaguchi, Y. and Maruyama, S., *The European Phys. J. D*, (1999), submitted.
17. Becke, A. D., *J. Chem. Phys.* **98**, 5648 (1993).
18. Lee, C., Yang, W., Parr, R. G., *Phys. Rev. B* **37**, 785 (1988).

19. Frisch, M. J., et al., *Gaussian 94 Revision E.1*, (Gaussian, Inc., Pittsburgh PA, 1995).
20. Maruyama, S., Anderson, L. R. and Smalley, R. E., *Rev. Sci. Instrum.* **61**, 3686 (1990).
21. Maruyama, S., Lee, M. Y., Haufler, R. E., Chai, Y. and Smalley, R. E., *Z. Phys. D* **19**, 409 (1991).
22. Maruyama, S., Anderson, L. R. and Smalley, R. E., *J. Chem. Phys.* **93**, 5349 (1990).
23. Maruyama, S., Yoshida, T., Kohno, M. and Inoue, M., *5th ASME/JSME Thermal Eng. Conf.*, San Diego, AJTE99-6513 (1999).
24. Maruyama, S., Kinbara, H., Hayashi, H. and Kimura, D., *Micro. Thermophys. Eng.* **1**, 39 (1997).
25. Journet, C., Maser, W. K., Bernier, P., Loiseau, A., de la Chapelle, M. L., Lefrant, S., Deniard, P., Lee, R., Fisher, J. E., *Nature* **388**, 756 (1997).